Phase locking effect and current reversals in deterministic underdamped ratchets

Maria Barbi* and Mario Salerno†
Dipartimento di Scienze Fisiche ''E.R. Caianiello,'' Università di Salerno, Italy
and INFM Unità di Salerno, I-84100 Salerno, Italy
(Received 13 March 2000)

We study the transport properties (currents) of deterministic underdamped ratchets in terms of phase locking dynamics. The occurrence of reverse currents is interpreted in terms of different stability properties of the periodic rotating orbits and is shown to exist also in the absence of bifurcations from chaos to periodic motion. We briefly discuss the effects of noise on this phase locked dynamics.

PACS number(s): 05.45.−a, 05.10.Gg

I. INTRODUCTION

The dynamics of a Brownian particle in asymmetric periodic potentials represents an interesting model for studying the transport properties of nonlinear systems in the presence of noise. In analogy with the ratchet mechanism considered by Feynman [1] in discussing the impossibility to extract work from thermodynamical equilibrium, these systems are also called ratchets. An interesting feature of the ratchet model is the possibility to use diffusion to convert an ac driving signal (either a multiplicative [2–5] or an additive [4,6,7] fluctuating term) into a net dc current corresponding to the unidirectional motion of the particle through the system (ratchet effect). This phenomenon has been observed in a variety of systems [8–10] and has been proposed as the mechanism underlying the functioning of biological motors [11–13]. The ratchet effect has also been used to design new experimental devices for physical [10,14–16] as well as biological [17,18] applications. A crucial role for the occurrence of the ratchet effect is played by the asymmetry of the potential and by the damping; the driving term keeps the system out of equilibrium while the noise seems to play, in the case of additive forcing, only a secondary role. The phenomenon can be indeed observed also in absence of noise, both in overdamped deterministic systems [7,19,20] and in underdamped chaotic ones [21]. This has recently sparked some interest in the study of deterministic ratchets. In particular, the case of a periodically forced underdamped particle with finite inertia in a periodic asymmetric potential was recently considered in Ref. [22]. For this system it was shown that there are several parameter ranges for which the particle can move with positive or negative velocity, as well as ranges for which the particle executes chaotic motion. The mechanism by which current reversal takes place was identified as the occurrence of a bifurcation from the chaotic to the periodic regime.

The aim of the present paper is to show that the transport properties of the underdamped deterministic ratchet can be interpreted in terms of phase locking phenomena, and the reverse currents can be ascribed to different stability properties of the rotating periodic orbits of the system. More precisely, we show that the presence of direct motion, either forward or backward, is always achieved when the time required for the particle to move from one well of the potential to another is commensurable with the period of the driver. Moreover, we show that, contrary to what was proposed in Ref. [22], current reversals can occur also in the absence of bifurcations from chaos to periodic motion.

The paper is organized as follows. In Sec. II we introduce the model and discuss its physical properties from a general point of view. In Sec. III we check our qualitative predictions by direct numerical integration. A complete analysis of the system behavior in the whole range of the forcing amplitude is done, and we present evidence of a phase locking mechanism. Current reversals which do not need any chaotic transitions are shown. We then describe the attracting orbits of the system in various cases and show how coexisting orbits with positive and negative velocity can give rise to hysteretic behavior. Finally, we briefly discuss the effects induced by noise and we draw our conclusions.

II. MODEL

Let us consider the motion of a particle in a spatially periodic potential with an asymmetric profile, subjected to a time-periodic force and to damping. The equation of motion, in dimensionless variables, is written as

$$\ddot{x}+b\dot{x}+\frac{dV(x)}{dt}=a\cos(\omega t), \tag{1}$$

where b is the friction coefficient, and ω and a, respectively, are the frequency and amplitude of the driver. To conform with previous studies, we take the same potential as in Ref. [22],

$$V(x)=C-\frac{1}{4\pi^2\delta}\left[\sin[2\pi(x-x_0)]+\frac{1}{4}\sin[4\pi(x-x_0)]\right], \tag{2}$$

where C and x_0 are introduced in order to have one potential minimum in $x=0$ with $V(0)=0$ [Fig. 1(a)] and $\delta=\sin(2\pi|x_0|)+\frac{1}{4}\sin(4\pi|x_0|)$. To understand the mechanism underlying the ratchet effect, it is convenient to analyze the system in its phase space. In the unperturbed case (i.e., b

*Email address: barbi@sa.infn.it
†Email address: salerno@sa.infn.it

 ©2000 The American Physical Society

$=0$, $a=0$) the phase space is similar to that of a simple pendulum, with separatrices dividing oscillating and rotating orbits as depicted in Fig. 1(b). When damping is introduced, the Hamiltonian character of the system is lost, and trajectories starting from different initial conditions fall down in the potential minima. Points $(n,0)$ in the phase space are in this case the only attractors of the corresponding dissipative system. Just as for the simple pendulum, the periodic driving will introduce chaos into the system via homoclinic splitting and transverse intersections of the separatrices, at particular parameter values. Stationary motion can also exist on special orbits which realize balance conditions between dissipated and gained energy. The qualitative behavior of the system can be described as follows. When a is much smaller than b, we can expect that small closed orbits near minima can be stable with periods commensurable with the period of the driver $T_\omega = 2\pi/\omega$. These motions will have zero average velocity and therefore zero current (i.e., no direct motion, either forward or backward). In the opposite case of very large a, the particle will also follow the forcing, this leading again to zero current. In the intermediate regime, chaos cannot be ignored and the situation becomes more complicated. Depending on the set of parameters, rotating orbits of the unperturbed system, corresponding to motions with positive or negative velocity, respectively, can give rise to attractors or repellers, which will contribute to the setup of either periodic or chaotic motion. In the first case a net current is expected, while in the second case erratic compositions of backward and forward motion (without net transport) should arise [22]. From a physical point of view, currents should be expected when the time required for the particle to move from one well of the potential to another becomes commensurable with the period of the driver, i.e., when the particle motion becomes locked to the external driver. In this case, the mean velocity of the particle should stay constant for all parameter values for which the locked solution is stable (locking range), and should be given by

$$\langle v \rangle = \frac{m}{n}\frac{T_{\rm pot}}{T_\omega} = \frac{m}{n}\frac{\omega}{2\pi}T_{\rm pot} = \frac{m}{n}v_\omega, \quad n \in N, m \in Z, \tag{3}$$

where $T_{\rm pot}$ is the spatial period of the potential (note that in our case $T_{\rm pot}=1$), and we call v_ω the fundamental locking velocity induced by the driver. Current reversals should appear in connection with stability changes of the rotating orbits in the superior and inferior part of the phase space. We shall check these predictions in the next section by direct numerical integration.

III. NUMERICAL RESULTS

To investigate the behavior of the system, we have made bifurcation diagrams by a stroboscopic recording of the first derivative $\dot{x}$ at subsequent crossing of the Poincaré section. An analogous plot reported in [22] refers to the window $a \in (0.075,0.086)$. Correspondingly, we obtain the plot of Fig. 2, on a larger parameter range, $a \in (0.06,0.12)$. Parameters ω and b are fixed to the values used by Ref. [22], $\omega = 0.67$, $b=0.1$, in order to allow direct comparison of the results. For each value of the parameter, after an initial transient, we record 400 values $\dot{x}(t_P)$ at times $t_P = n_P T_\omega$, where n_P is an integer. Periodic orbits of period kT_ω $(k \in N)$ correspond to k crossing points at Poincaré section, and therefore to k values of $\dot{x}$ at the corresponding a. A complete analysis of the whole range of interest is depicted in Fig. 3, where we present bifurcation diagrams for different intervals of the forcing amplitude a. Figure 3(a) refers to the small a range, while the other three plots cover, with a decreasing

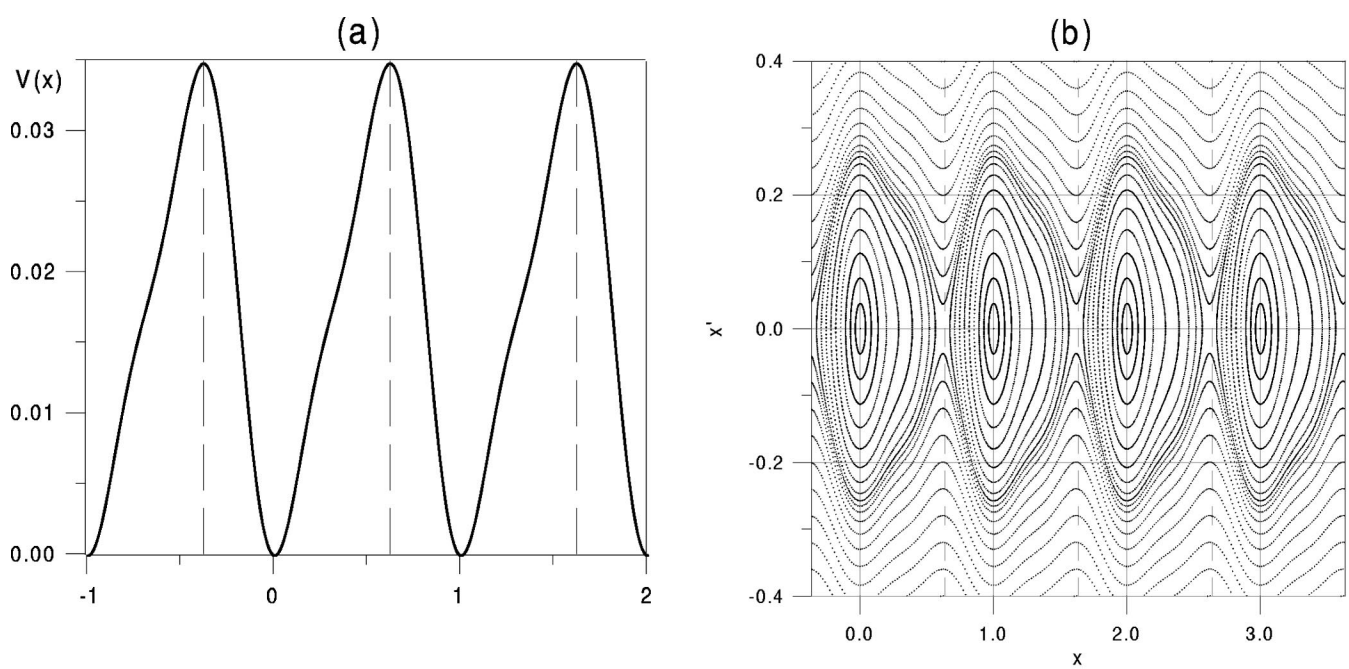

FIG. 1. (a) The periodic potential $V(x)$ used, with parameters $x_0 = -0.19$, $C=0.0173$ as in Ref. [22]. (b) The phase space of the unperturbed system, i.e., system (1) with $a=0$, $b=0$. A series of closed and rotating orbits are shown. Dashed grid lines correspond to potential maxima. All variables are dimensionless.

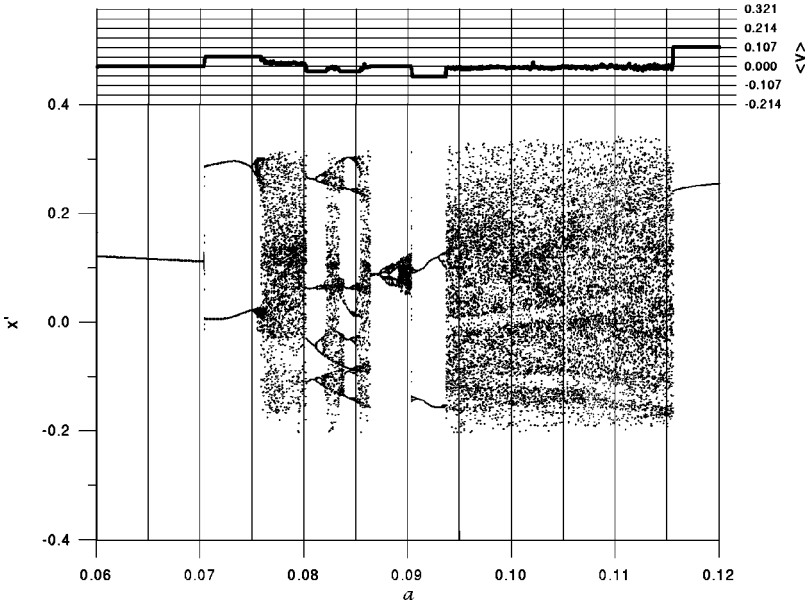

FIG. 2. Bifurcation diagram (lower graph) and mean velocity (upper graph) in the range of the forcing parameter $a \in (0.06,0.12)$, including the interval discussed in Ref. [22]. The other system parameters are $b=0.1$ and $\omega=0.67$. Grid lines in the velocity plot correspond to multiples of half the driver-induced locking velocity, which is $v_{\omega} \cong 0.107$ with our choice of parameters. All variables here and in the following graphs are dimensionless.

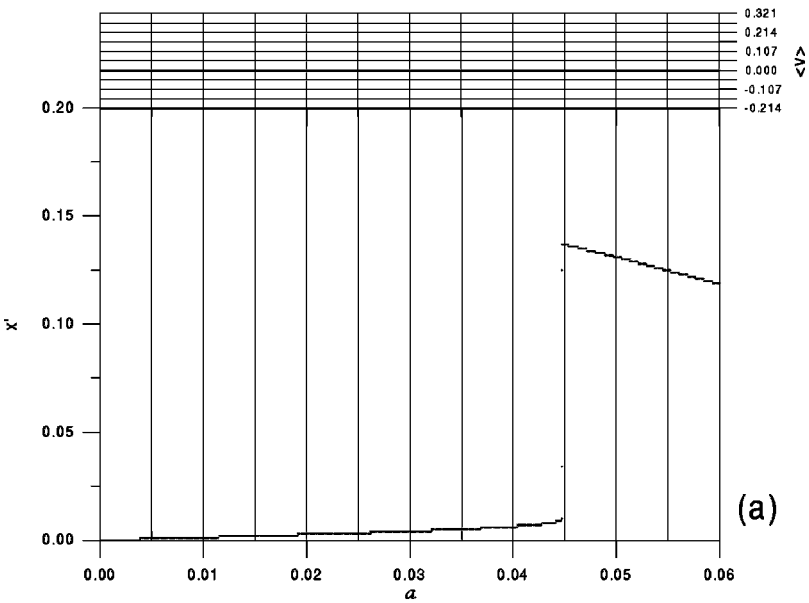

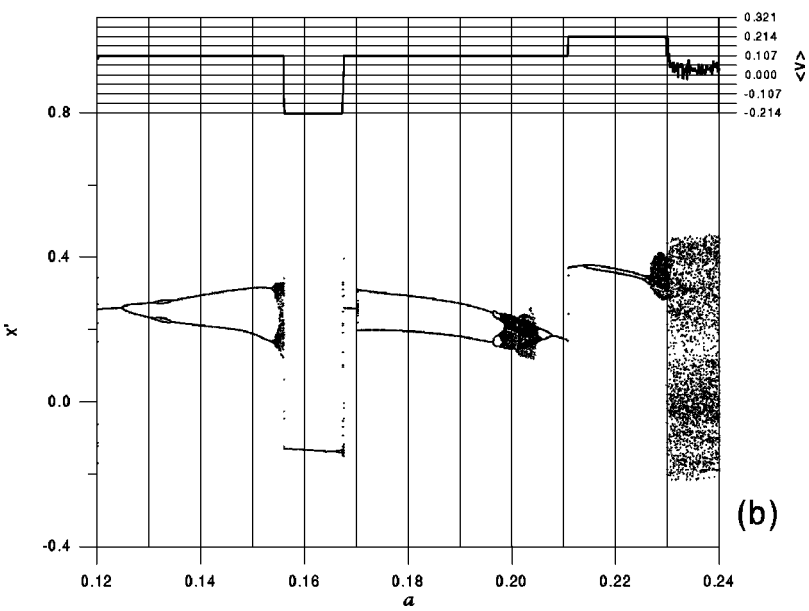

FIG. 3. Bifurcation diagrams (lower graphs) and mean velocity plots (upper graphs) in four different ranges of the forcing parameter a, which complete the region shown in Fig. 2 to cover the whole range of interest. Same settings as in Fig. 2 are used. The considered intervals are (a) $a \in (0,0.06)$; (b) $a \in (0.12,0.24)$; (c) $a \in (0.24,0.9)$; (d) $a \in (0.9,8)$.

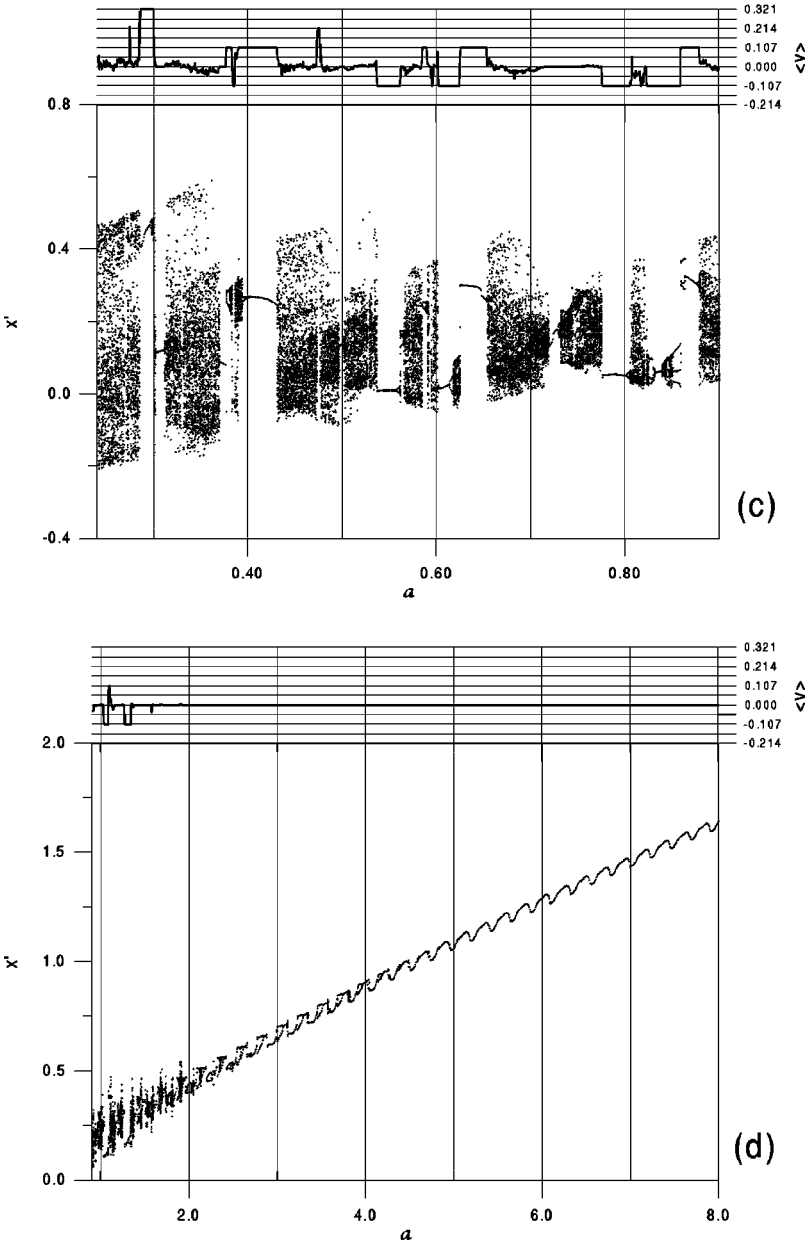

FIG. 3. *(Continued).*

level of precision, the range from the last value of Fig. 2 up to large a values. In the upper part of each plot of Fig. 2 and Fig. 3, we give the corresponding mean velocity $\langle v \rangle$ as a function of a. The velocity is time-averaged over 300 forcing periods, with a time step of $T_\omega/1000$.

The general behavior of the system, depicted in Figs. 2 and 3, corresponds to the predictions of the preceding section. One of the relevant features of these plots is, as also mentioned in [22], the presence of a wide series of current reversals in a large interval of the parameter, with regular and chaotic regions. Chaotic orbits appear around $a=0.75$ and can be found up to values of about 2. For larger values of a, a regular, periodic motion with $\langle v \rangle = 0$ dominates. In the opposite limit, i.e., for values of a tending to zero ($a < 0.06$), the particle displays again regular motion with periodicity T_ω and mean velocity $\langle v \rangle = 0$. In the intermediate range, alternate periodic orbits with periodicity T_ω, $2T_\omega$, $3T_\omega$, $4T_\omega$, and $8T_\omega$ can be easily recognized (see, for instance, regions near $a=0.12$, 0.18, 0.86, 0.081, and 0.085, respectively). In these regular regions, the mean velocity of the particle agrees with Eq. (3), i.e., we have a constant velocity locked to values $\langle v \rangle / v_\omega = 0$, $\pm 1/2$, ± 1, ± 2, and even 1/4 (near $a=0.08$) and 3 (near $a=0.3$). Note that in contrast with our results, the current shown in Fig. 2 of Ref. [22] is not constant in the phase locking regions. This is probably due to the method of computing averages. After having computed, as we did, time averages, the authors of Ref. [22] also performed an average on initial conditions. This procedure is useful in the presence of noise, but in the deterministic case it is unnecessary. Furthermore, it can mask the phase locking effect by mixing orbits originating from initial conditions which correspond to different attractors basins: as we will see, in fact, such coexisting attractors exist, and correspond to different locked velocities.

For what concerns specifically current reversals, let us now consider more in detail the region $a \in (0.14, 0.18)$ [Fig. 3(b)]. In this region we observe two subsequent reversals, from $\langle v \rangle = v_\omega$ to $\langle v \rangle = -2v_\omega$ and back, *without chaotic*

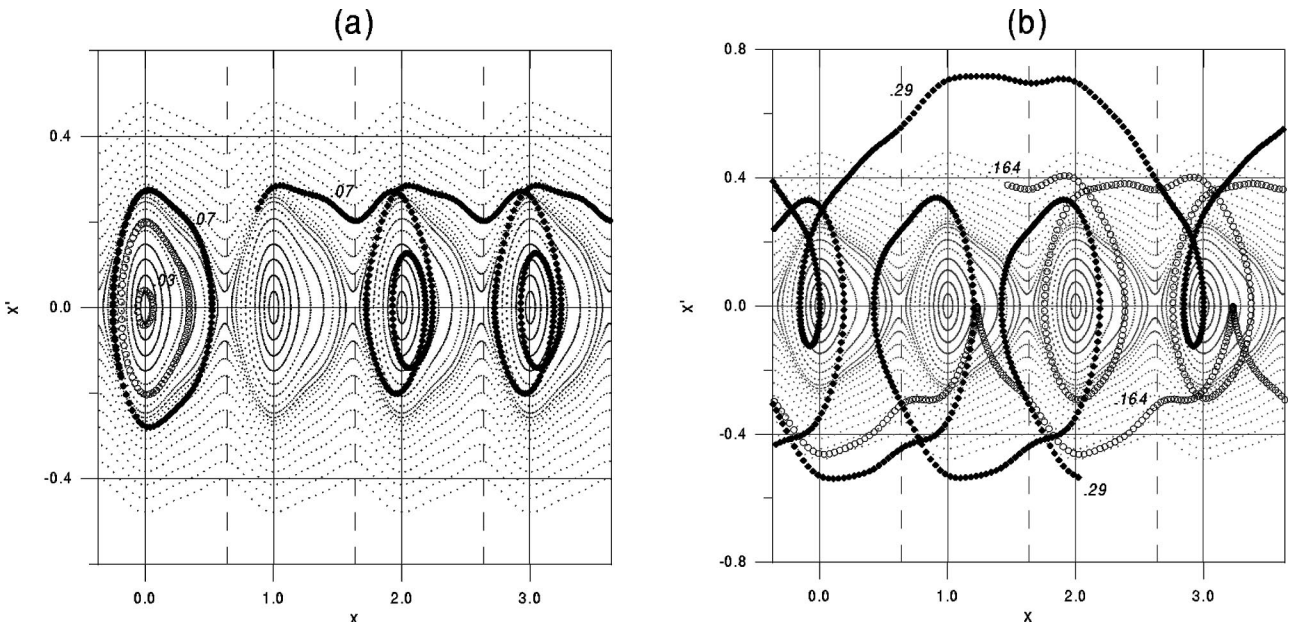

FIG. 4. Some attracting orbits of the system (1) in the cases $a=0.03$ [(a), open circles]; 0.07 [(a), full diamonds]; $a=0.164$ [(b), open circles]; 0.29 [(b), full diamonds]. Underlying unperturbed phase-space structure is shown on the back for comparison. Some orbits are only partially shown for readability. Variables are dimensionless.

transition. The bifurcation paths leading to these reversals do not produce in fact any chaotic orbit but just period doubling without reaching chaos, as it can also be seen from the regular behavior of the average velocity. The same can be observed, e.g., in the region $a \in (0.85,0.87)$, where a switch from two period-$3T_\omega$ orbits, with velocity $\pm v_\omega$, takes place even without period doubling.

In order to check our predictions about the role of closed and rotating trajectories in the system behavior, we show in Fig. 4 some of the typical attracting orbits of the system in the cases $a=0.03,0.07$ [Fig. 4(a)] and $a=0.164,0.29$ [Fig. 4(b)] obtained by letting particles evolve starting from different initial conditions. As suggested in the preceding section, we find that nonzero velocities correspond to orbits which can be roughly described as a composition of parts which are near the closed orbits of the unperturbed system and parts close to the external ones (they are more and more deformed as the value of the parameter a increases). External paths allow the particle to jump to neighboring wells. For small values of a (as, e.g., for $a=0.03$), only internal orbits are stabilized, while for increasing values of the parameter, particles spend an increasing amount of time near the external paths. Each time that the particle goes near external orbits, it jumps forward of backward and moves one or more potential steps. At $a=0.07$, the particle can jump only once each two periods, so that its periodicity will be of $2T_\omega$ and its velocity of $v_\omega/2$. For larger values of a, the particle can jump more than one step, thus increasing velocity. Interestingly, at $a=0.07$ we observe *contemporaneously* the presence of this moving orbit with a periodic closed orbit with

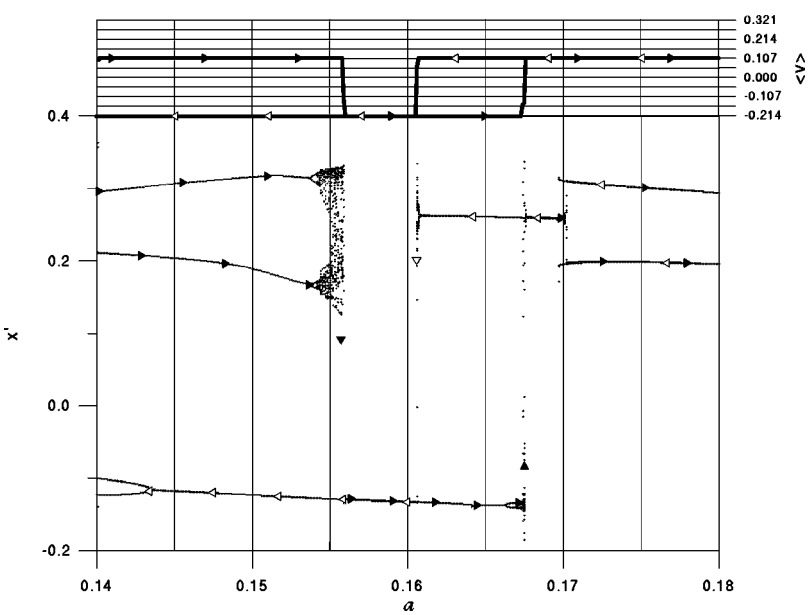

FIG. 5. Bifurcation diagram (lower graph) and mean velocity (upper graph) obtained by first increasing the driving amplitude a from 0.14 to 0.18 and then decreasing it back to the initial value. Typical hysteresis is evident in the velocity behavior. Correspondingly, the bifurcation diagram shows the contemporary presence of different stable orbits, as discussed in the text. Small arrows superimposed on both graphs indicate the direction of the amplitude variation: increasing for full arrows, decreasing for open ones.

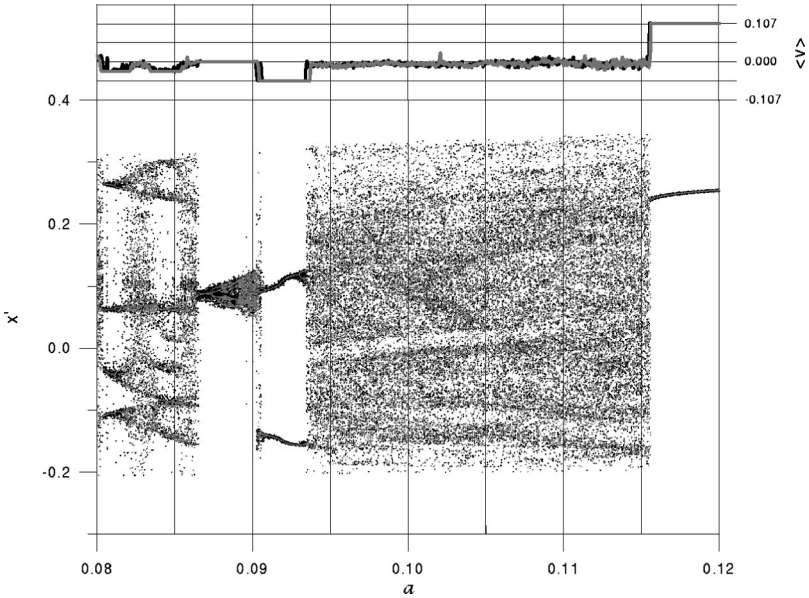

FIG. 6. Effects of the addition to the model of a noise term with $D=10^{-7}$. The considered interval is $a\in(0.08,0.12)$. Mean velocity and bifurcation plot for the case $D=0$ are also shown for comparison (blue line and dots).

zero velocity. This means that, for some values of the forcing amplitude, different attractors can coexist [21] and one expects this to be true also for *forward* and *backward* trajectories at particular values of the bifurcation parameter.

This is actually what we observe, for instance, at $a=0.164$ and at $a=0.29$, as shown Fig. 4(b). In the first case, the forward motion is due to a periodic orbit which turns around the unperturbed minima and goes to the next well in one period T_ω, so that the resulting velocity is v_ω; the backward motion has larger velocity $-2v_\omega$ and still corresponds to a period-T_ω orbit, but where the particle jumps two wells at a time. The case of $a=0.29$ is similar, with forward velocity $3v_\omega$ and backward $-v_\omega$, and again period T_ω. From these results we can thus deduce that chaotic transitions are not needed for current reversals: instead, one could switch directly from positive to negative velocity with a small change of the parameter, and even by simply forcing the particle to fall down on different attractors by changing its initial conditions.

The fact that different attractors can coexist in some region of the parameter space implies hysteretic phenomena. To see hysteresis, we have performed bifurcation patterns in both directions, i.e., by first increasing and then decreasing the bifurcation parameter *a*. This was done for three regions, namely $a\in(0.055,0.075)$, i.e., in correspondence to the first period doubling observed (see Fig. 2); $a\in(0.14,0.18)$, of Fig. 3(b), where current reversals have been identified; and in the region considered in Ref. [22], i.e., $a\in(0.074,0.086)$. In the last case, where a period doubling route to chaos takes place, we do not observe any hysteresis, while it can be clearly observed in the other two cases. Bifurcation and mean velocity plots corresponding to the interval (0.14,0.18) are reported in Fig. 5, from which we see that hysteresis affects also the mean velocity behavior and its origin is related to the presence of coexisting orbits, as, e.g., in the region (0.140,0.155).

In closing this section, we shall briefly discuss the effects induced by noise on the deterministic ratchet effect. To this end we added a stochastic term $+2D\xi(t)$ to the right-hand side of Eq. (1), where $\xi(t)$ is white noise and D is the noise intensity. We show one bifurcation diagram and the corresponding mean velocity plot, obtained for intensity $D=10^{-7}$, in Fig. 6. Mean velocity for the case $D=0$ is also shown in blue color for comparison. Noise leads to a broadening of the bifurcation pattern, with a little influence on the average velocity. Indeed, larger locked regions appear to be preserved with no relevant change in width, while smaller ones show a decreasing stability. By increasing noise intensity, stable orbits are more and more perturbed, until they become completely indistinguishable from stochastic motion. At $D=10^{-6}$, we found that in the same range of Fig. 6 almost all the periodic regions disappeared; nevertheless, one still gets locking in the last, largest one ($a\geqslant 0.115$), which still corresponds to a constant velocity. We remark that a noise intensity $D=10^{-6}$ in model (1) corresponds, e.g., to thermal noise at room temperature for a system with mass $m\sim 200$ k a.m.u.$\sim 3.3\times 10^{-19}$ g, spacing $L\sim 8$ nm, and a potential barrier of $8kT$, as it can be evaluated by inverting the transformation used in [22] back to dimensional variables. These are the typical orders of magnitude for the case of kinesin [4].

IV. CONCLUSIONS

In this paper we have considered the ratchet effect in deterministic underdamped systems with asymmetric potentials and periodic forcing. We showed that the occurrence of a net motion in the system is always related to phase locked dynamics. The phenomenon of current reversals was described and ascribed to different stability properties of the perturbed rotating orbits of the system. We showed that, in contrast with previous results, current reversals can happen also in the absence of chaos-to-order transitions. Hysteretic current reversals were also found and their occurrence was related to the coexistence of different periodic attractors. We also investigated the role of noise on the deterministic dynamics. We found that noise has no positive effects on the stabilization of periodic orbits of the locked regions, i.e., on the setting up of direct or inverse current in the system. It is, how-

ever, quite important that deterministic phase locked ratchet dynamics can survive even at high levels of noise intensity. It is precisely the robustness of this phenomenon which makes the ratchet effect an interesting possible mechanism by which biological systems can take advantage of noisy environments to produce net motion.

ACKNOWLEDGMENTS

M.B. wishes to thank the EC and the University of Salerno for financial support. Financial support from INFM and the European grant LOCNET (Contract No. HPRN-CT-1999-00163) is acknowledged.

[1] R. P. Feynman, R. B. Leighton, and M. Sands, *The Feynman Lectures on Physics* (Addison-Wesley, Reading, MA, 1966), Vol. 1.
[2] A. Ajdari and J. Prost, C. R. Acad. Sci., Ser. II: Mec., Phys., Chim., Sci. Terre Univers **315**, 1635 (1992).
[3] M. O. Magnasco, Phys. Rev. Lett. **71**, 1477 (1993).
[4] M. Bier and R. D. Astumiano, Phys. Rev. Lett. **72**, 1766 (1994).
[5] C. R. Doering, Nuovo Cimento D **17**, 685 (1995).
[6] C. R. Doering, Physica A **254**, 1 (1998).
[7] P. Hänggi and R. Bartussek, in *Nonlinear Physics of Complex Systems*, Lecture Notes in Physics Vol. 476, edited by J. Parisi, S. C. Muller, and W. Zimmermann (Springer, Berlin, 1996).
[8] L. P. Faucheux *et al.*, Phys. Rev. Lett. **74**, 1504 (1995).
[9] L. Gorre-Talini, J. P. Spatz, and P. Silberzan, Chaos **8**, 650 (1998).
[10] O. Sandre *et al.*, Phys. Rev. E **60**, 2964 (1999).
[11] R. D. Vale and F. Oosawa, Adv. Biophys. **26**, 97 (1990).
[12] N. J. Cordova, B. Ermentrout, and G. F. Oster, Proc. Natl. Acad. Sci. USA **89**, 39 (1992).
[13] F. Jülicher, A. Ajdari, and J. Prost, Rev. Mod. Phys. **69**, 1269 (1997).
[14] L. Gorre, E. Ioannidis, and P. Silberzan, Europhys. Lett. **33**, 267 (1996).
[15] C. Kettner *et al.*, Phys. Rev. E **61**, 312 (2000).
[16] D. Ertas, Phys. Rev. Lett. **80**, 1548 (1998).
[17] L. Gorre-Talini, S. Jeanjean, and P. Silberzan, Phys. Rev. E **56**, 2025 (1997).
[18] J. S. Bader *et al.*, Proc. Natl. Acad. Sci. USA **96**, 13 165 (1999).
[19] J.-F. Chauwin, A. Ajdari, and J. Prost, Europhys. Lett. **27**, 421 (1994).
[20] J.-F. Chauwin, A. Ajdari, and J. Prost, Europhys. Lett. **32**, 373 (1995).
[21] P. Jung, J. G. Kissner, and P. Hänggi, Phys. Rev. Lett. **76**, 3436 (1996).
[22] J. L. Mateos, Phys. Rev. Lett. **84**, 258 (2000).